Jouberin localizes to collecting ducts and interacts with nephrocystin-1

Lorraine Eley[1], Christos Gabrielides[1], Matthew Adams[2], Colin A. Johnson[2], Friedhelm Hildebrandt[3] and John A. Sayer[1]

[1]*Institute of Human Genetics, International Centre for Life, Newcastle University, Newcastle Upon Tyne, UK;* [2]*Section of Ophthalmology and Neurosciences, Wellcome Trust Brenner Building, Leeds Institute of Molecular Medicine, St James's University Hospital, Leeds, UK and* [3]*Departments of Pediatrics and of Human Genetics, University of Michigan, Ann Arbor, Michigan, USA*

Joubert syndrome and related disorders are autosomal recessive multisystem diseases characterized by cerebellar vermis aplasia/hypoplasia, retinal degeneration and cystic kidney disease. There are five known genes; mutations of which give rise to a spectrum of renal cystic diseases the most common of which is nephronophthisis, a disorder characterized by early loss of urinary concentrating ability, renal fibrosis, corticomedullary cyst formation and renal failure. Many of the proteins encoded by these genes interact with one another and are located at adherens junctions or the primary cilia and or basal bodies. Here we characterize Jouberin, a multi-domain protein encoded by the *AHI1* gene. Immunohistochemistry with a novel antibody showed that endogenous Jouberin is expressed in brain, kidney and HEK293 cells. In the kidney, Jouberin co-localized with aquaporin-2 in the collecting ducts. We show that Jouberin interacts with nephrocystin-1 as determined by yeast-2-hybrid system and this was confirmed by exogenous and endogenous co-immunoprecipitation in HEK293 cells. Jouberin is expressed at cell-cell junctions, primary cilia and basal body of mIMCD3 cells while a Jouberin-GFP construct localized to centrosomes in subconfluent and dividing MDCK cells. Our results suggest that Jouberin is a protein whose expression pattern supports both the adherens junction and the ciliary hypotheses for abnormalities leading to nephronophthisis.

Kidney International (2008) **74,** 1139–1149; doi:10.1038/ki.2008.377; published online 16 July 2008

KEYWORDS: nephronophthisis; collecting ducts; cilia; cyst

Correspondence: *John A. Sayer, Institute of Human Genetics, International Centre for Life, Central Parkway, Newcastle Upon Tyne NE1 3BZ, UK. E-mail: j.a.sayer@ncl.ac.uk*

Received 7 February 2008; revised 13 May 2008; accepted 20 May 2008; published online 16 July 2008

Joubert syndrome and related disorders (JBTS)[1] are a group of inherited recessive neurological diseases characterized by cerebellar vermis aplasia/hypoplasia and retinal degeneration.[2,3] The syndrome is characterized neuroradiologically by the 'molar tooth sign' secondary to cerebellar vermis aplasia, prominent superior cerebellar peduncles, and a deep interpeduncular fossa.[4] Patients exhibit developmental delay, mental retardation, loss of muscle tone, irregular breathing patterns, and abnormal eye movements.[1] In addition to these core features patients may exhibit cystic kidney disease and nephronophthisis (NPHP), these patients being termed JBTS type B or cerebello-oculo-renal syndrome.[5] The monogenic causes of JBTS have recently been discovered. There are now five known genes implicated (*NPHP1*, *AHI1*, *NPHP6/CEP290*, *RPGRIP1L/NPHP8*, and *MKS3/TMEM67*) and a further two loci (*JBTS1/CORS1* on chromosome 9q34.3 and *JBTS2/CORS2* on chromosome 11p12-11q33.3)[5–7] have been well described. Mutations in all of these genes, or at these loci, may all give rise to renal cystic disease, most commonly NPHP. NPHP is characterized by an early loss of urinary concentration ability, progressive interstitial fibrosis, tubular basement membrane disruption, and corticomedullary cyst formation. It is the most common cause of renal failure in children and young adults.[8]

AHI1 (Abelson helper integration-1), a gene that encodes for the protein Jouberin, is mutated in 10–15% of cases of the autosomal recessive disease JBTS.[9] Expression studies to date are limited to brain expression of Jouberin mRNA[10,11] and expression studies in haematopoietic cells.[12] The domain structure of the Jouberin protein, which includes an Src homology 3 (SH3) domain and six or seven WD40 domains (in human and mouse, respectively) is in keeping with other adapter proteins.

NPHP1 mutations are the most common genetic cause of NPHP, accounting for 25% of all cases of NPHP.[13,14] Mutations are commonly a homozygous gene deletion (in 85% of cases) or a heterozygous deletion with a single point mutation on the second allele.[15] Recently, mutations in *NPHP1* have been found in a subset of patients with JBTS[16] and probably account for 1–2% of the total of all JBTS patients.[9] On the basis of mutation analysis of *AHI1* and

NPHP1, an epistatic interaction between Jouberin and nephrocystin-1 has recently been postulated.[17] Domain analysis of the nephrocystin-1 protein reveals a coiled-coil domain together with a SH3 domain. Nephrocystin-1 is known to interact with p130Cas (alias BCAR1) through its SH3 domain, binding to the PXXP motif.[18] Because nephrocystin proteins and Jouberin possess multiple interaction domains and coiled-coil domains this allows speculation that these proteins form multiple protein–protein interactions and function as a large complex. In addition, the pattern of subcellular localization of nephrocystin proteins, with a predominantly cilial/basal body localization also points toward a functional complex of nephrocystin proteins and implicates the primary cilia in disease pathogenesis.[19]

Given the variable renal phenotype and the genetic overlap with other NPHP-causing genes, we investigated the expression pattern and protein interactions of Jouberin in renal cells, in order to try and understand possible mechanisms of renal disease in JBTS. Intriguingly, many of the nephrocystin proteins, together with polycystins, BBS proteins and MKS proteins, collectively known as 'cystoproteins' because of their renal cystic phenotype if mutated, have been shown to localize to distinct cell compartments. These include primary cilia, centrosomes, and basal bodies thus suggesting a role for these structures in cystic kidney disease.[20,21] This ciliary localization of nephrocystin proteins may be combined with a cell–cell junction localization.[13,22] Data concerning whole kidney expression of nephrocystins are extremely sparse due to a lack of specific antibodies. In particular, the expression pattern of Jouberin within the kidney and its molecular interactions remain unknown. Here we demonstrate that Jouberin is expressed in human and mouse brain and kidney, in addition to the ciliated renal epithelial cell lines human embryonic kidney (HEK293), murine inner medullary collecting duct (mIMCD3), and Madin–Darby canine kidney (MDCK) cells. We demonstrate that Jouberin interacts with nephrocystin-1 and that Jouberin colocalizes at cell–cell contacts with β-catenin. Expression of a Jouberin–green fluorescent protein (GFP) construct demonstrates a centrosomal localization and in confluent mIMCD3 cells we demonstrate that Jouberin associates with acetylated α-tubulin in the primary cilium. Finally, in human kidney, Jouberin expression is seen in renal collecting duct cells, colocalizing with aquaporin-2 (AQP2).

RESULTS

Jouberin is a multidomain protein

Sequence analysis of the Jouberin peptide sequence reveals a high degree of conservation between human and mouse Jouberin, with amino-acid identity 80%. The main difference between these two species is the presence of 140 N-terminal amino acids in the human Jouberin, which are absent from the murine Jouberin. Domain analysis (http://smart.embl-heidelberg.de/ and http://www.ch.embnet.org/software/COILS) reveals that both human and murine N-terminal sequences encode a coiled-coil domain. Both human and murine Jouberin and nephrocystin-1 proteins possess a SH3 domain which may bind to target proteins through sequences containing proline and hydrophobic amino acids.[23] Finally, the human Jouberin protein contains six WD40 domains, whereas the murine Jouberin has seven WD40 domains (Figure 1a).

Yeast 2-hybrid interactions between Jouberin and nephrocystin-1

Direct yeast 2-hybrid experiments were performed between the full-length human nephrocystin-1 and full-length Jouberin and a series of Jouberin subclones (Figure 1b). The SH3 domain subcloned from nephrocystin-1 was also used for these studies. Results (shown in Figure 1c) demonstrate that nephrocystin-1 interacts with Jouberin. This interaction persists while using subclones of Jouberin, which contain WD40 domains and the SH3 domain from nephrocystin-1. When bait and prey are reversed, the Jouberin clone containing WD40 domains 5 and 6 (subclone Jouberin_C) is the only positive interaction (Figure 1c). Positive controls for these interaction studies include confirming an yeast interaction between nephrocystin-1 and the SH3-binding domain of nephrocystin-4 and between nephrocystin-1 and p130Cas, which has a PXXP motif, known to bind to the SH3 domain.[24] Appropriate negative controls were used to exclude self-activation of the yeast constructs (Figure 1c).

Jouberin is endogenously expressed in brain and kidney

Reverse transcriptase-PCR analysis of Jouberin mRNA confirms its expression in human brain and kidney (Figure 2a), mouse brain and kidney (Figure 2b), and in renal epithelial cell lines HEK293, mIMCD3, and MDCK cells (Figure 2c). Using a novel anti-Jouberin antibody (Ab737) directed toward a peptide at the C-terminus of Jouberin (Figure 1a), Western blotting revealed bands of approximately 160 kDa in size in HEK293, mIMCD3, and MDCK cells, respectively, as well as adult mouse kidney and brain (Figure 3a). There are some >250 kDa bands seen in HEK293 and MDCK cells, which are peculiar to these cell lines and are likely to be nonspecific. An additional smaller Jouberin isoform ($\sim$120 kDa) is seen in mIMCD3 cells and mouse kidney. Database searches do not predict a Jouberin isoform of this length, suggesting this may be a novel kidney-specific isoform of Jouberin. Peptide preabsorption was able to block detection by the antibody of the expected ($\sim$165 kDa) and smaller ($\sim$120 kDa) isoforms; demonstrating specificity of the antibody, and Western blotting using preimmune sera was negative (Figure 3a). The specificity of the anti-Jouberin Ab737 antibody was also confirmed using overexpression of Jouberin–GFP in HEK293 cells. The anti-Jouberin Ab737 detected the endogenous band in addition to a higher molecular weight band corresponding to the GFP fusion protein. Anti-GFP antibodies detected the same weight band only in transfected cells (Figure 3b). Using an alternative anti-Jouberin (Ab7367) antibody directed toward a peptide

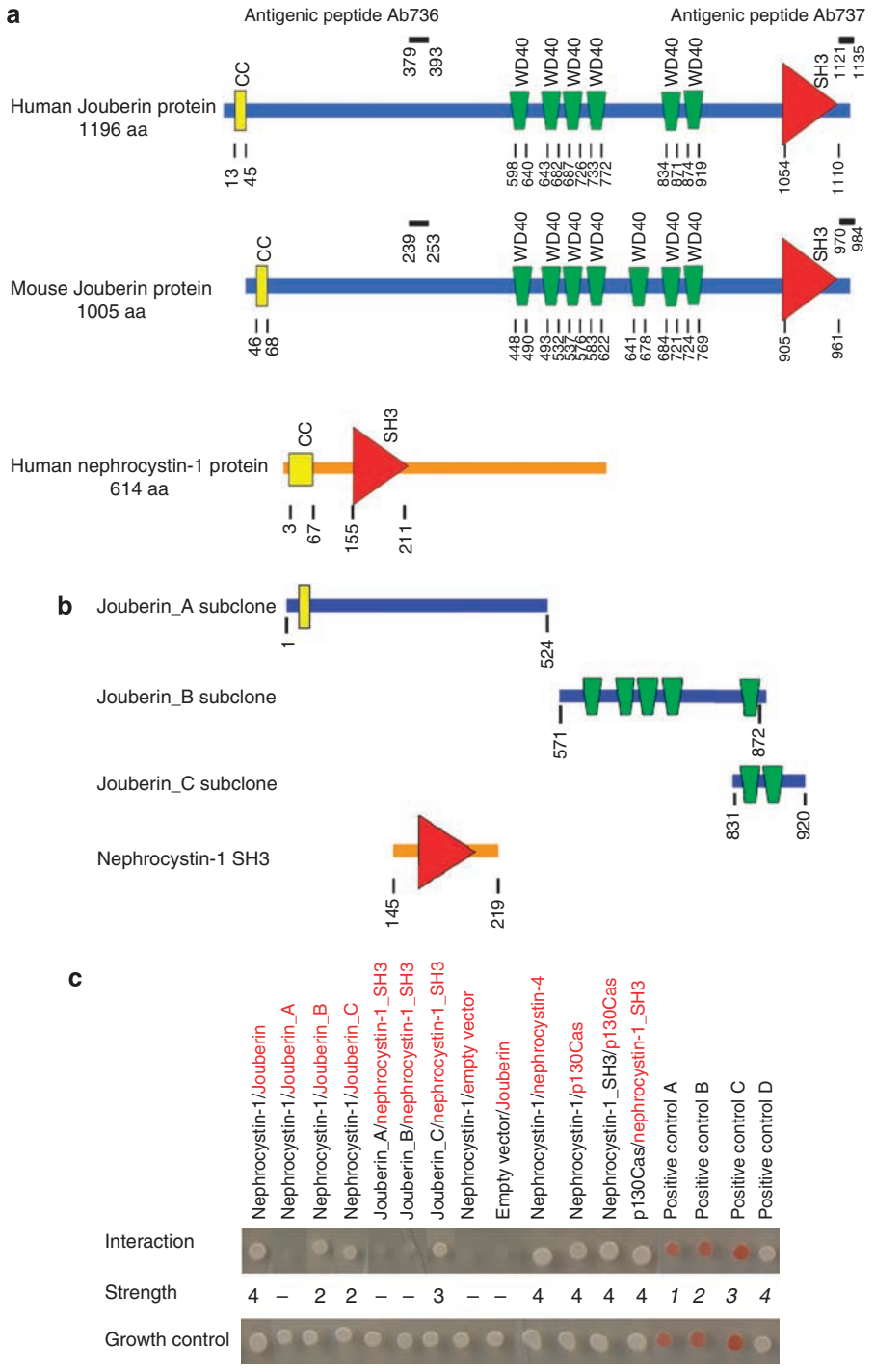

Figure 1 | Domain structure of Jouberin and yeast 2-hybrid interaction studies. (**a**) Schematic representation of the human and mouse isoforms of Jouberin and human nephrocystin-1 protein with their predicted protein domains (using http://smart.embl-heidelberg.de/ and http://www.ch.embnet.org/software/COILS). Each protein sequence is depicted by a straight line with known protein domains represented by colored boxes at their relative positions in the sequence, with amino-acid numbers given for the start and end of each domain. For Jouberin, the antigenic sequences used to generate antibodies Ab736 and Ab737 are also shown as black bars. CC, coiled coil; WD40, WD40 repeats; SH3, Src homology-3. (**b**) Schematic representation of subclones of Jouberin (Jouberin_A, Jouberin_B, and Jouberin_C) and the SH3 domain from nephrocystin-1 protein. The amino-acid residues of each clone are shown, in comparison to the full-length clones shown in (**a**). Known protein domains within the subclones are shown as in (**a**). (**c**) In yeast 2-hybrid direct interaction analysis, human nephrocystin-1 as bait interacts with human Jouberin as prey. This interaction is partially mapped with nephrocystin-1 failing to interact with Jouberin_A, but interacting with Jouberin_B and Jouberin_C. In reciprocal interactions Jouberin_C (bait) is able to interact with SH3 domain of nephrocystin-1 (Nephrocystin-1_SH3), implicating the WD40 domains of Jouberin and the SH3 domain of nephrocystin-1 in this interaction. Empty-vector controls are shown. Positive controls show that nephrocystin-1 interacts with nephrocystin-4 and p130Cas. Interaction strength controls *1–4* are also shown. Strength of the interaction is scored by colony growth on triple drop out medium, as compared to controls. Control for colony growth is shown on medium deficient in leucine (–Leu) and tryptophan (–Trp). Red color in certain control colonies is expected to occur upon starvation for specific amino acids.

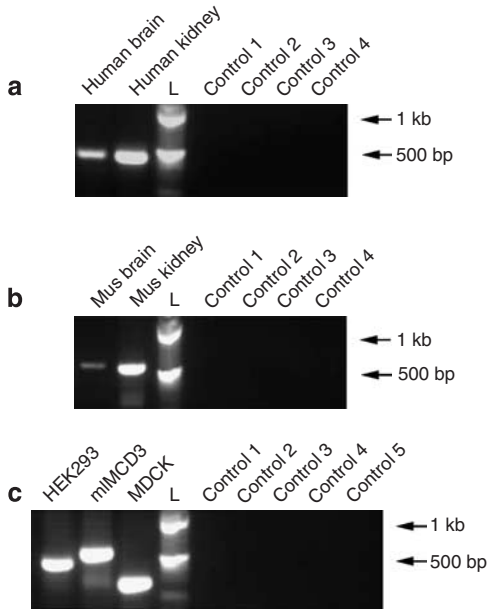

Figure 2 | RT-PCR expression of Jouberin. RT-PCR products are visualized on a 0.8% agarose gel using Jouberin-specific (and species specific) oligonucleotide primers. (**a**) RT-PCR products of the expected size (474 bp) are seen using human brain and kidney total RNA as template. (**b**) RT-PCR products of the expected size (578 bp) are seen using mouse brain and kidney total RNA as template. For (**a**, **b**), negative controls 1 and 2 omitted RT enzyme for brain and kidney samples, respectively, controls 3 and 4 omitted RNA. (**c**) RT-PCR products of the expected sizes (474, 578, and 329 bp, respectively) are seen using total RNA extracted from HEK293, mIMCD3, and MDCK cells as templates. Negative controls 1, 2, and 3 omitted RT enzyme for each template, respectively, controls 4 and 5 omitted RNA. L, DNA size ladder (100 bp ladder; New England Biolabs, Ipswith, MA).

corresponding to amino-acid positions 379–393 in human Jouberin (Figure 1a), Western blotting also reveals bands of approximately 160 kDa in MDCK, HEK293, and mIMCD3 cells. Preimmune sera do not detect these bands (Figure 3c).

Coimmunoprecipitation of Jouberin and nephrocystin-1

In order to confirm yeast interactions we used exogenous expression of Jouberin and nephrocystin-1 cDNA constructs in HEK293 cells. The interaction between nephrocystin-1 and human Jouberin was confirmed using coimmunoprecipitation of V5 and Flag-tagged constructs. Flag-tagged nephrocystin-1 was co-precipitated with V5-tagged Jouberin using anti-Flag antibodies, and confirmed using reciprocal coimmunoprecipitation using anti-V5 antibody (Figure 4a and b). This interaction was also demonstrated using a murine Jouberin construct, which is identified at a lower molecular weight than the human Jouberin construct (Figure 4c). This difference in mass corresponds to a predicted difference in molecular weight of 22 kDa between the human and mouse proteins encoded by the exogenously expressed cDNA constructs. As a positive control for our system of exogenous overexpression we confirmed by coimmunoprecipitation the known interaction between nephrocystin-1 and p130Cas (data not shown). We further confirmed the interaction between Jouberin and nephrocystin-1 using endogenous expression in HEK293 cells and coimmunoprecipitation. Using anti-Jouberin conjugated to protein A, nephrocystin-1 coimmunoprecipitates with Jouberin (Figure 4d). Using site-directed mutagenesis, we prepared a Jouberin construct containing a missense mutation, R830W. This *AHI1* mutation has previously been identified in JBTS patients with *NPHP1* or *NPHP6* mutations,[17] but its functional significance at the protein level is unknown. Using coimmunoprecipitation experiments in HEK293 cells, we confirm that this mutation alone is not sufficient to abrogate the interaction. Coexpression of Jouberin-R830W and nephrocystin-1 proteins are still able coimmunoprecipitate together (Figure 4e).

Endogenous Jouberin is expressed at cell–cell contacts in renal epithelium and is a part of the cilial/centrosomal complex

Endogenous expression of Jouberin was observed in the cytoplasm and cell–cell contacts in polarized mIMCD3 cells using anti-Jouberin Ab737 antibody (Figure 5a). The staining toward Jouberin is highly specific, fully blocked by preincubation of the primary antibody with its peptide, and preimmune serum gave no signal (Figure 5a). Double staining with Jouberin antibody and an antibody directed toward β-catenin, an adherens junction-associated protein, demonstrates partial colocalization in mIMCD3 cells (Figure 5b). Anti-Jouberin Ab736 did not work well for immunofluorescence studies.

Using a GFP-tagged Jouberin construct transfected MDCK cells of low confluence revealed diffuse cytoplasmic staining, together with specific staining resembling basal bodies, colocalizing with γ-tubulin, a basal body marker, in a cell during interphase (Figure 5c). In a cell undergoing mitosis, Jouberin–GFP can be seen at the spindle poles (Figure 5d). In confluent, post-mitotic mIMCD3 cells, left 96 h past the point of confluency to allow optimal ciliogenesis, anti-Jouberin antibodies demonstrate punctuate staining that is associated with acetylated α-tubulin (Figure 6).

Endogenous Jouberin is expressed in human renal collecting duct cells

Immunofluorescent staining using Jouberin Ab737 on human kidney sections containing renal cortex and medulla identified a subset of nephron segments expressing Jouberin (Figure 7a). Omitting Jouberin antibody and using preimmune sera demonstrates specificity of the antibody (Figure 7a). Jouberin staining nephron segments resembled collecting ducts. Therefore, using double staining with Jouberin and AQP2 antibodies, we demonstrate Jouberin expression in collecting duct segments with AQP2 staining at the apical plasma membranes and subapical regions (Figure 7b and c). Jouberin staining in collecting duct cells appears near plasma membranes, both basolaterally and apically. The staining pattern of Jouberin is restricted to collecting ducts, with neighboring (AQP2 negative) tubules demonstrating an absence of Jouberin expression. Control sections, which

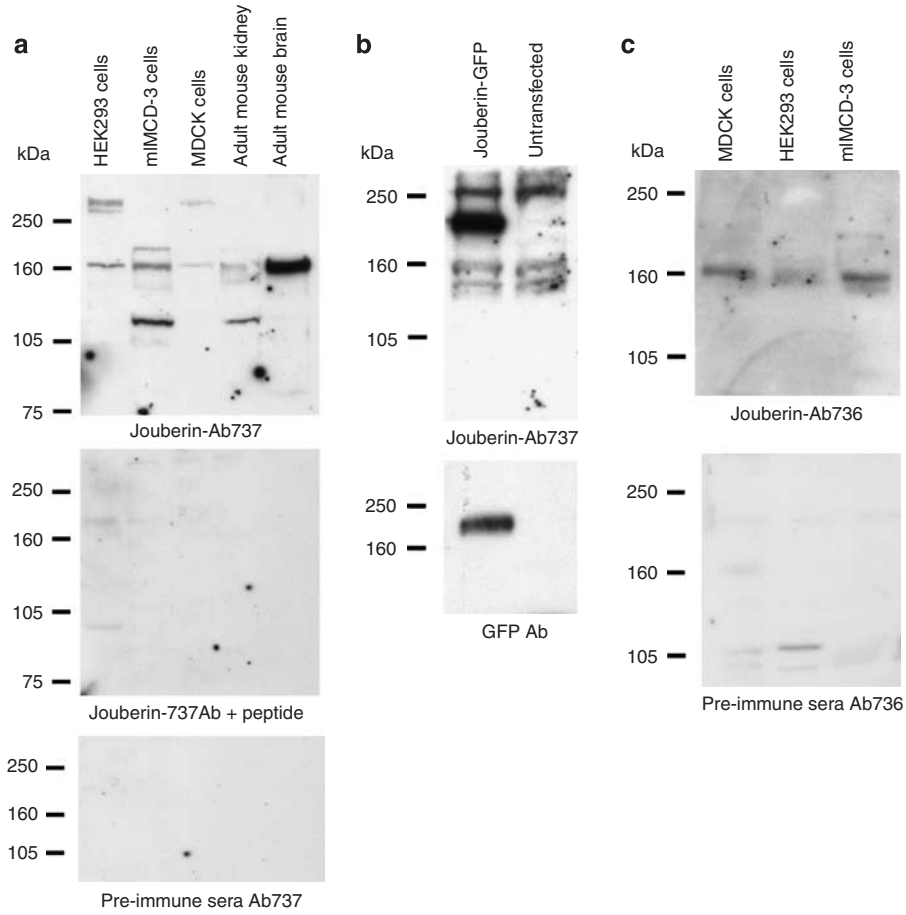

Figure 3 | Endogenous Jouberin expression and characterization of novel anti-Jouberin antibody. (**a**) Western blotting using the Jouberin (Ab737) antibody reveals bands of approximately 165 kDa in cell lines HEK293, mIMCD3, and MDCK, and mouse brain and kidney tissue. A smaller isoform (~120 kDa) is noted in mIMCD3 and mouse kidney. Incubation of antibody with peptide blocks detection of the ~165 kDa bands and the smaller isoforms. In addition, no bands are seen in the preimmune control. (**b**) Using HEK293 cells Jouberin–GFP was overexpressed. Cell lysates probed with anti-Jouberin antibodies revealed endogenous expression and an additional higher molecular weight band corresponding to Jouberin–GFP fusion protein (absent in control untransfected cells; upper panel). Anti-GFP antibody confirmed the expression of Jouberin–GFP in transfected cells (lower panel). (**c**) Western blotting using the Jouberin (Ab736) antibody reveals bands of approximately 165 kDa in cell lines MDCK, HEK293, and mIMCD3. These bands are not seen in the preimmune control.

omitted primary Jouberin or AQP2 antibodies, revealed no staining, excluded cross-reaction of secondary antibodies.

DISCUSSION

Using a novel antibody, we have established the presence of endogenous renal expression of Jouberin protein. This is in keeping with the kidney phenotype of JBTS with renal involvement (JBTS type B/cerebello-oculo-renal syndrome), which includes urinary concentration defects, NPHP and cystic kidneys.

Mutations in *AHI1*, the gene encoding for Jouberin, account for around 10–15% of patients with JBTS,[3] with renal involvement occurring as a variable phenotype.[25–27] Other JBTS causing gene defects also display a variable phenotype, with *NPHP1* mutations giving a prominent renal phenotype and *NPHP6* mutations giving a prominent retinal phenotype.[26,28] This variable phenotype may be due to different tissue expression of the protein but also may be secondary to oligogenicity, as discussed below.

Using yeast interaction studies we demonstrate that nephrocystin-1 interacts with Jouberin. Furthermore, this interaction was present using both full-length clones and using subclones of Jouberin, which contained WD40 domains 1–5 and WD40 domains 5–6, thus partially mapping the interaction. Coimmunoprecipitation experiments confirmed this interaction between nephrocystin-1 and Jouberin, both in exogenous expression systems and using endogenous coimmunoprecipitation (Figure 4). Given that mutations in either *NPHP1* or *AHI1* may be seen in JBTS patients, our results strengthen the hypothesis that there is a functional interaction between nephrocystin-1 and Jouberin. This is relevant to mechanisms of human disease, as a possible genetic (epistatic) interaction has been described between *NPHP1* and *AHI1* in JBTS patients. Tory *et al.* describe five patients with *NPHP1* mutations whom also carried a R830W mutation in *AHI1*,[17] which interestingly lies just before the fifth WD40 domain of Jouberin. These patients had more prominent neurological manifestations of

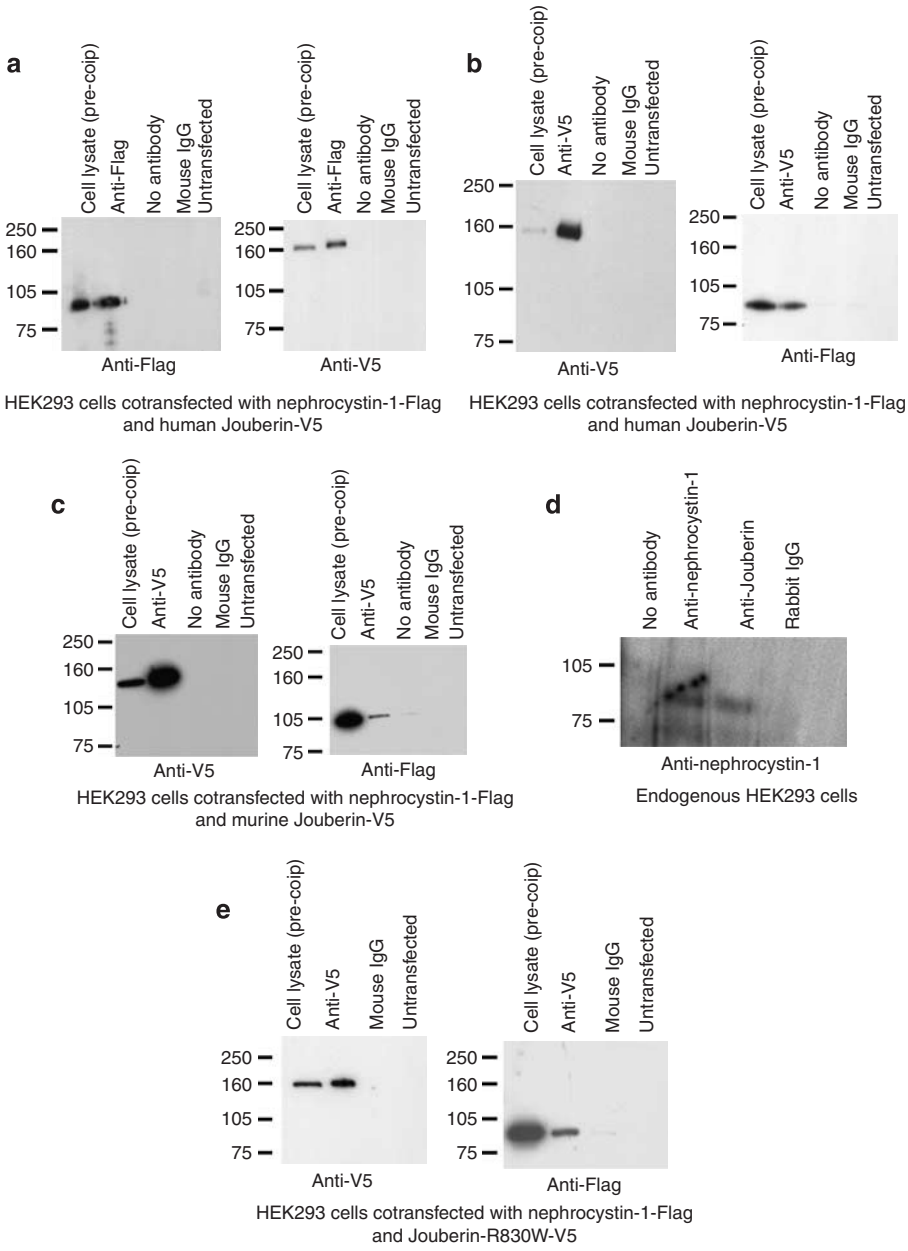

Figure 4 | Coimmunoprecipitation of Jouberin with nephrocystin-1. (**a**, **b**) Human nephrocystin-1 interacts with human Jouberin. HEK293 cells were co-transfected with constructs containing human nephrocystin-1 tagged with Flag and human Jouberin tagged with V5. (**a**) Using anti-Flag on protein G, detection with anti-Flag showed that human nephrocystin-1 was able to immunoprecipitate nephrocystin-1 (left panel) and detection with anti-V5 antibody showed that human nephrocystin-1 could coimmunoprecipitate human Jouberin (right panel). (**b**) Using anti-V5 on protein G, detection with anti-V5 showed that human Jouberin was able to immunoprecipitate Jouberin (left panel) and detection with anti-Flag antibody showed that human Jouberin could coimmunoprecipitate human nephrocystin-1 (right panel). (**c**) Human nephrocystin-1 interacts with mouse Jouberin. HEK293 cells were co-transfected with constructs containing human nephrocystin-1 tagged with Flag and mouse Jouberin tagged with V5. Using anti V5 on protein G, detection with anti-V5 showed that mouse Jouberin was able to immunoprecipitate Jouberin (left panel) and detection with anti-Flag antibody showed that mouse Jouberin could coimmunoprecipitate human nephrocystin-1 (right panel). (**d**) Human nephrocystin-1 interacts with Jouberin in HEK293 cells. Lysates from untransfected HEK293 were immunoprecipitated using anti-nephrocystin-1 on protein A (lane 2), and using anti-Jouberin on protein A (lane 3). (**e**) Nephrocystin-1 interacts with Jouberin-R860W-mutant protein. HEK293 cells were co-transfected with constructs containing human Nephrocystin-1 tagged with Flag and Jouberin-R830W tagged with V5. Using anti-V5 on protein G, detection with anti-V5 showed that mutated Jouberin-R830W was able to immunoprecipitate itself (left panel) and detection with anti-Flag antibody showed that mutated Jouberin-R830W was able to coimmunoprecipitate nephrocystin-1 (right panel). In all experiments negative controls including untransfected cells, no antibody on protein G or A and mouse/rabbit IgG substituting the detecting antibody.

the disease.[17] WD40 domains seem to be functionally important for the interaction between Jouberin and nephrocystin-1. The Jouberin R830W missense mutation is not sufficient to prevent the interaction between Jouberin and nephrocystin-1 when these proteins are exogenously expressed.

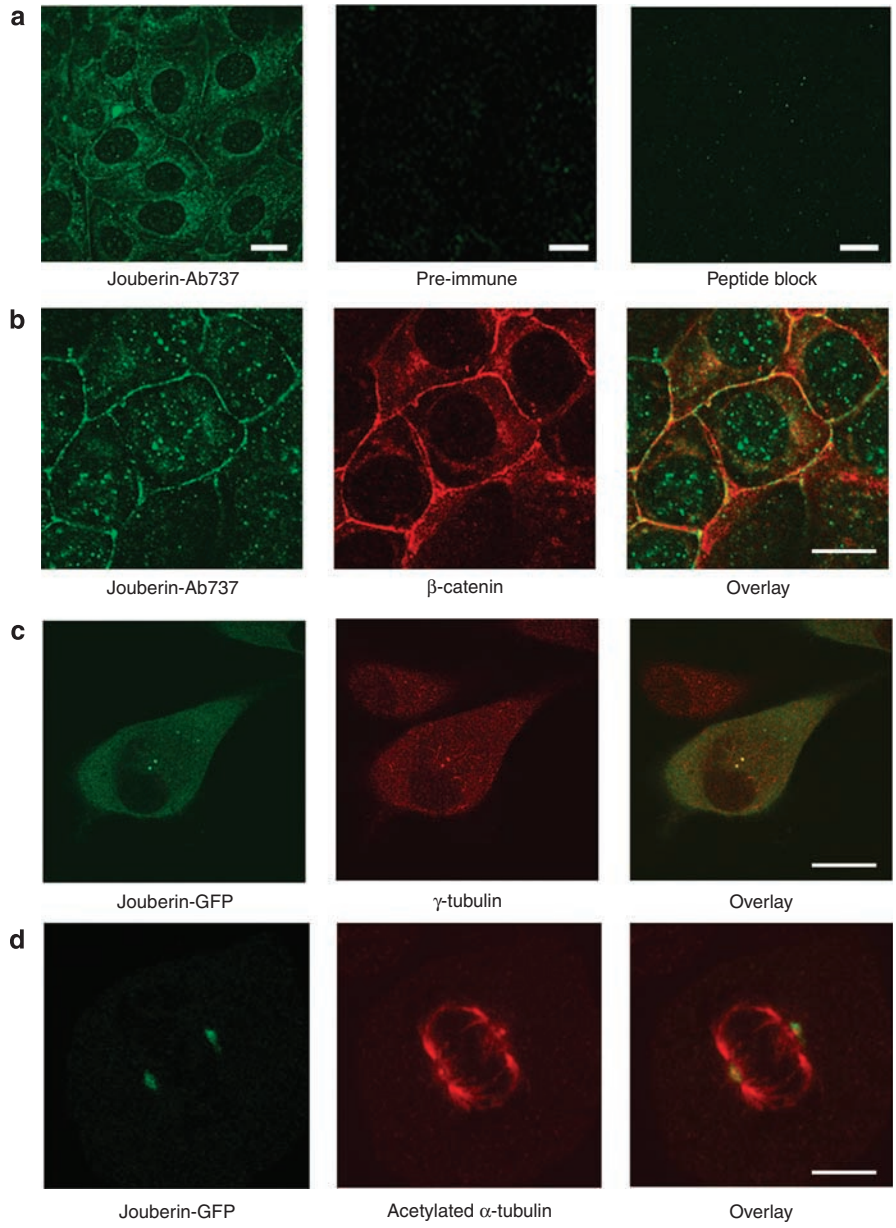

Figure 5 | Jouberin is expressed both at the adherens junction and centrosomal complex in renal epithelial cells. mIMCD3 cells were grown in a confluent monolayer (for 5 days) before fixation. Midcell confocal sections were examined after methanol fixation and stained with (**a**) anti-Jouberin (green) with preimmune serum staining and peptide-blocking controls shown below. (**b**) Co-staining with anti-Jouberin (green) and anti-β-catenin antibody (red). MDCK cells transfected with Jouberin–GFP cDNA were fixed in paraformaldehyde. (**c**) Transfected cell (in interphase) counterstained with γ-tubulin (red), to highlight centrosomes. (**d**) A transfected cell (undergoing mitosis) is counterstained with acetylated α-tubulin antibodies (red). Bar = 10 μm.

Given we have shown Jouberin expression at cell–cell contacts, with colocalization with β-catenin, this suggests that Jouberin, like nephrocystin-1[29] and nephrocystin-4,[22] is an adherens junction-associated protein. This adherens junction role for nephrocystin proteins is supported by known interaction between nephrocystin-1 and p130Cas (alias BCAR1) and PTK2B.[30] Colocalization of Jouberin with β-catenin may also implicate Jouberin in functional pathways including Wnt signalling,[31] which may play key roles in determining proliferation rates, polarity, and organogenesis.

Like other nephrocystins, Jouberin expression was not limited to one subcellular compartment, as we also show a centrosomal and ciliary localization. Jouberin–GFP colocalizes with centrosomal structures and its localization during cell division appears dynamic, in a similar manner to inversin[32,33] and nephrocystin-6.[28] In confluent cells we are able to show association in a punctuate manner with acetylated α-tubulin in the axoneme of the primary cilia. This observation implicates the pathogenesis of JBTS is caused by a defect in primary ciliary structure or function, in a similar manner to other 'cystoproteins'.[19] Thus, like

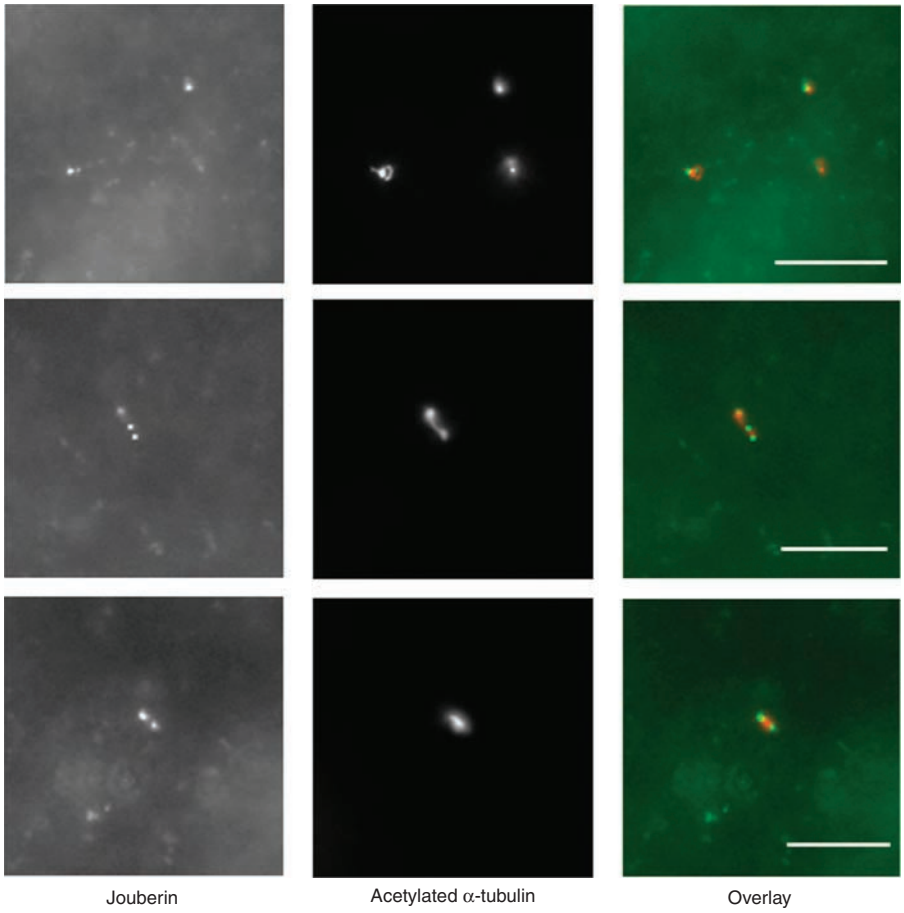

Figure 6 | Jouberin colocalizes with acetylated α-tubulin in the primary cilia of renal epithelial cells. mIMCD3 cells were grown on glass coverslips for 96 h past confluency before fixation in paraformaldehyde. Above cell surface epifluorescent images were captured after staining with anti-Jouberin (left) and acetylated α-tubulin (middle) and demonstrates an association with ciliary structures (right: Jouberin, green; acetylated α-tubulin, red). Bar = 5 μm.

nephrocystin-4,[22] Jouberin is a protein whose expression pattern supports both an adherens junction hypothesis and a ciliary hypothesis for mechanism leading to NPHP.[19]

Finally, in human kidney, we are able to show that Jouberin is expressed in renal tubules. This may not be surprising to note, given the renal phenotype, but the study of Jouberin expression in human renal tissue is completely novel. Furthermore, expression of Jouberin was limited to tubules expressing AQP2, namely the renal collecting duct cells. This is highly topical as inherited renal cystic diseases, such as neophronophthisis, are associated with a loss of ability to concentrate urine.[34–38] Typically, a patient with NPHP will develop symptoms of polydipsia and polyuria at the age of 4–6 years, related to the underlying defect in urine concentration ability and a failure to concentrate urine following a water deprivation test is a characteristic finding in NPHP.[8] In compensation for this inability to concentrate urine, the vasopressin V2 receptor and APQ2 protein are overexpressed *in vivo* in mouse models of cystic kidney disease.[39–41] This concentrating defect has previously been attributed to the progressive renal impairment or the disruption of renal medullary anatomy by cysts. However, such concentrating defects seem to precede collecting duct cyst formation in animal models of cystic kidney disease. In patients with NPHP, cyst formation and end-stage renal failure is typically reached at 12–13 years of age, many years after symptomatic urinary concentrating defects have been noted. These clinical observations, combined with various mouse models of cystic kidney disease, including NPHP (the *pcy* mouse[20]) have lead to the use of vasopressin receptor antagonists as a therapeutic agent to treat cystogenesis.[42]

Given the collecting duct distribution of Jouberin we have demonstrated, together with its 'adherens junction' role in cell culture models, we hypothesize that Jouberin defects may compromise both epithelial integrity and cell–cell signalling. Defective adherens junctions within the collecting duct would reduce the osmotic gradient for effective water reabsorption leading to polyuria. A more limited expression of Jouberin along the nephron may account for the milder cystic phenotype seen in NPHP kidneys, as compared to autosomal-dominant polycystic kidney disease, where cyst formation may occur at any segment, as polycystin-1 and -2 proteins are expressed along the entire length of the nephron.

In conclusion, we characterize the JBTS protein Jouberin in terms of a novel protein–protein interaction with

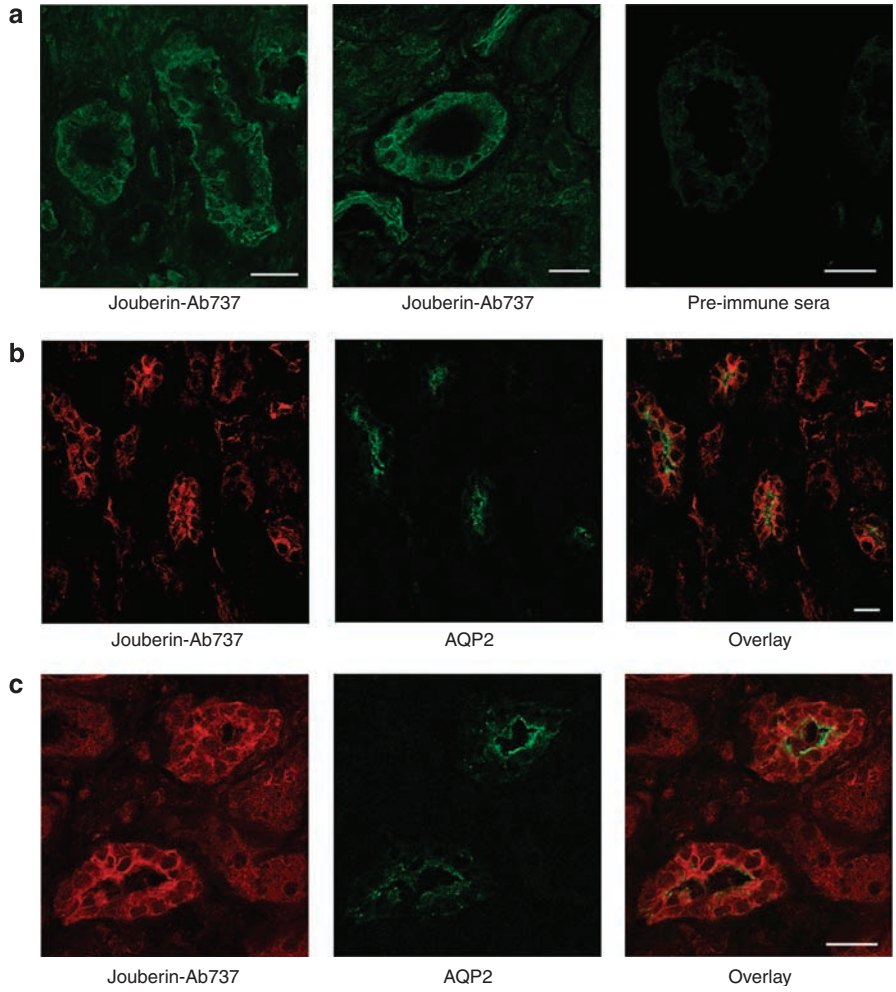

Figure 7 | Jouberin is expressed in human renal collecting duct cells. Human kidney sections were stained with anti-Jouberin (Ab737). (**a**) Single antibody-stained sections demonstrate Jouberin expression in a subset of nephron segments. A negative control using preimmune sera for Ab737 is shown. Bar = 20 μm. (**b**, **c**) Double antibody-stained sections using anti-Jouberin and anti-aquaporin-2 (AQP). Overlayed images show that Jouberin expression is limited to collecting duct segments, stained positively with AQP2. Bar = 20 μm.

nephrocystin-1, subcellular localization in cultured renal cells, and tissue distribution within the human kidney. Models of *AHI1* knockdown are now required to test functional roles of Jouberin in these specific locations.

MATERIALS AND METHODS

Real-time-PCR of Jouberin from whole tissues and cell culture lines

Total RNA was obtained from whole mouse kidney, whole mouse brain, and cell lines HEK293, MDCK, and mIMCD3 cells using TRIZOL (Sigma, Gillingham, Dorset, UK) extraction reagent. Human kidney and brain total RNA was obtained from a commercial library (Clontech, Saint-Germain-en-Laye, France). RNA (2 μg) was reverse transcribed according to the protocol using SuperScript III Reverse Transcriptase (Invitrogen, Paisley, UK). Negative controls omitted reverse transcriptase.

PCR used HotStartTaq DNA polymerase (Qiagen, Crawley, West Sussex, UK) with 2 μl reverse-transcribed RNA in a 20 μl reaction. Oligonucleotide primer concentration was 0.5 μM. PCR amplification was over 30 cycles. Gene-specific oligonucleotide primers for human, mouse, and *Canis* Jouberin were designed from available database sequences (Ensembl). For human Jouberin primers were 5-TTGG AACCCAGAAACAGGAG-3 and 5-ATCTCTTGAGCGGTCAGCAT-3, predicted product size 474 bp. For mouse Jouberin primers were 5-AG ATCGCACAGGAAATGGAG-3 and 5-AAGCACTTGGGATGAACTG G-3, predicted product size 578 bp, for *Canis* Jouberin primers were 5-CCGCTCATCACATTCAACAC-3 and 5-CCGCTCATCACATTCAA CAC-3, predicted product size 329 bp. PCR products were analyzed using agarose gel electrophoresis.

Jouberin antibody generation

Rabbit anti-Jouberin polyclonal antibody (Ab737) was generated using a synthetic peptide approach by CovalAb, Cambridge, UK. Purified synthetic peptide spanning human Jouberin amino acids 1121–1135 (Figure 1) was used to raise the immune response in rabbits. A second rabbit anti-Jouberin polyclonal antibody (Ab736) was prepared in a similar manner, using and antigenic peptide spanning human Jouberin amino acids 379–393 (Figure 1). Immunopurification of antipeptide antibodies using a sepharose column was carried out.

Tagged protein generation

Human and murine Jouberin and human nephrocystin-1 sequence was PCR amplified from IMAGE clones (IMAGE: 3908210, 6467369,

and 4284129, respectively) then subcloned into pENTR/D-TOPO (Invitrogen). Direct sequencing verified sequence fidelity and reading frame. Clones were then switched to DEST 53 (N-terminal GFP) and/or DEST (N-terminal V5) using the Gateway system (Invitrogen). Full-length human nephrocystin and p130Cas both tagged with 3XFLAG were purchased from GeneCopoeia, Berlin, Germany, site-directed mutagenesis of Jouberin to create the R830W missense mutation was carried out using mutagenic primers 5′-AGAATTATGGATCTC**t**GGATATTAGTAGCAAG-3′ and 5′-CTTG CTACTAATATCC**a**GAGATCCATAATTCT-3′ and PCR protocols as per QuikChange site-directed mutagenesis (Stratagene, La Jolla, CA, USA). Direct sequencing of clones was performed to verify the presence of the mutation.

Western analysis of endogenous and exogenous Jouberin

MDCK, mIMCD3, HEK293, adult mouse kidney, adult mouse brain, and HEK293 transfected with human Jouberin DEST 53 (N-terminal GFP) were solubilized in protein extraction buffer (4 M urea, 125 mM Tris pH6.8, 4% SDS, 10% glycerol, 5% β-mercaptoethanol, and 0.02% bromophenol blue). Protein samples were heated to 95 °C for 5 min and then run out on 6% SDS–polyacrylamide gel electrophoresis. Samples were then electrophoretically transferred from the gel to Amersham, Buckinghamshire, UK Hybond-C-extra nitrocellulose. Membranes were blocked in 5% milk (Marvel, Premier Foods, St Albans, UK) in Tris-buffered saline Tween-20 for 1 h at room temperature (RT). Endogenous and exogenous Jouberin was detected by incubating with the rabbit anti-Jouberin antibody (Ab737 or Ab736; 1:100) in blocking buffer for 1 h at RT. Three 15 min washes Tris-buffered saline Tween-20 were carried out at RT. The secondary antibody was polyclonal swine anti-rabbit conjugated to horseradish peroxidase (HRP; Dako, Ely, Cambridgeshire, UK) diluted 1:2000 in blocking buffer. Exogenous Jouberin was also detected with anti-GFP conjugated to HRP (Santa Cruz, CA, USA) 1:5000. Membranes were developed using the super signal west Dura extended duration substrate system (Pierce Biotechnology, Rockford, IL, USA). For the blocking/competition control Jouberin antibody was combined with a fivefold (by weight) excess of blocking peptide and then incubated for 2 h at RT. Jouberin antibody preimmune serum diluted in blocking buffer to the same final concentration as AHI1 antibody was used as a further control.

Coimmunoprecipitation

HEK293s were transiently co-transfected with either human Jouberin-V5 and human nephrocystin-1-3XFLAG or mouse Jouberin-V5 and human nephrocystin-1-3XFLAG using Lipofectamine 2000. After 24 h cells were washed in phosphate-buffered saline (PBS), pelleted, and lysed in NP-40 buffer (150 mM sodium chloride, 0.5% NP-40, 50 mM Tris pH 7.4, phenylmethanesulphonylfluoride, and protease inhibitors). The lysate was centrifuged for 20 min at 10,000 *g* at 4 °C and the supernatant was precleared with protein G sepharose beads (GE Healthcare, Giles, Buckinghamshire, UK). After removal of protein G the supernatant was then incubated overnight with protein G and 1 μg of either anti-V5 (Invitrogen), anti-Flag (Sigma), or mouse IgG (Sigma) at 4 °C. The beads were washed extensively in lysis buffer and bound proteins resolved by 6% SDS–polyacrylamide gel electrophoresis as described above. Flag-tagged proteins were detected as described above using with anti-Flag-conjugated to HRP (Sigma) 1:10,000 and V5-tagged proteins were detected with anti-V5 conjugated to HRP (Invitrogen) 1:5000.

For endogenous coimmunoprecipitation studies, HEK293 cells were lysed in NP-40 buffer. The lysate was centrifuged for 20 min at 10,000 *g* at 4 °C and the supernatant was precleared with protein A (Pierce). After removal of protein A the supernatant was then incubated overnight with protein A and 2 μg of either rabbit anti-Jouberin, rabbit anti-nephrocystin-1 (Santa Cruz), or rabbit IgG at 4 °C. The beads were washed extensively in lysis buffer and bound proteins resolved by 6% SDS–polyacrylamide gel electrophoresis as described above. Nephrocystin-1 was detected using rabbit anti-nephrocystin-1 (Santa Cruz) 1:500 and anti-rabbit HRP 1:2000 (Dako).

Yeast direct interaction studies

Clones of human Jouberin, human nephrocystin-1, and domain subclones were used as bait/prey, fused to the *GAL4* DNA-binding domain in the pDEST32 vector as bait and/or fused to the Gal4 activation domain fusion vector (pDEST22; Invitrogen). Plasmids were transformed into competent MaV203 yeast cells using the lithium acetate method (as described in[28]). Interaction experiments were performed using –His, –Leu, and –Trp-deficient medium containing 25 mM 3-aminotriazole. Colony growth was compared to two negative controls (respective plasmids without insert) and four positive control yeast strains for different interaction strength (as previously described[28]).

Exogenous expression and immunohistochemistry

MDCK cells were transfected with the human Jouberin–GFP construct using a nucleofector (Amaxa Biosystems, Cologne, Germany). A total of 1×10^6 cells were transfected with 5 μg of cDNA construct. Cells were incubated at 37 °C for 48 h before fixing in 4% paraformaldehyde. mIMCD3 cells were grown to confluence for endogenous Jouberin expression and fixed in 100% methanol for 2 min at −20 °C or 4% paraformaldehyde in PBS for 1 h then permeabilized using 1 × PBS/0.5% Triton X-100 only for paraformaldehyde-fixed tissue. All cells were blocked for 1 h at RT in 10% bovine serum albumin in PBS. Endogenous Jouberin was detected with anti-Jouberin (Ab737; 1:100) overnight at 4 °C. Cells transfected with Jouberin–GFP were double stained with either mouse-acetylated α-tubulin (1:1000; Sigma) or mouse anti- γ-tubulin (1:100; Sigma) for 1 h at RT. Cells were washed three times with PBS then incubated with the appropriate secondary antibody; fluorescein-conjugated goat anti-rabbit (Stratech Scientific Ltd, Suffolk, UK; 1:200) for 1 h at RT or Alexa Fluor 594 donkey anti-mouse (1:200; Invitrogen) for 1 h at RT. Human kidney sections (from the healthy pole of nephrectomy specimens following informed consent and full ethical approval) were flash frozen in liquid nitrogen and sectioned. Sections were fixed in methanol for 2 min at −20 °C before antibody staining. For single staining, following blocking with 10% bovine serum albumin in PBS, Jouberin was detected using (rabbit) anti-Jouberin (Ab737; 1:100) overnight at 4 °C and fluorescein isothiocyanate goat anti-rabbit secondary antibodies (1:200; Stratech). For double staining, following blocking with 10% bovine serum albumin in PBS, Jouberin was detected using (rabbit) anti-Jouberin (Ab737) (1:100) overnight at 4 °C and secondary anti-rabbit Cy3 (Sigma), raised in sheep (1:200) for 1 h at RT. Goat primary AQP2 antibodies (Santa Cruz; 1:250; 1 h at RT) were used to detect collecting duct cells, secondarily detected with donkey anti-goat FITC (Jackson Immuno Research, Westgrove, PA, USA; 1:100) for 1 h at RT. Control sections omitted Jouberin or AQP2 primary antibodies. Additional controls for anti-Jouberin antibodies used rabbit preimmune sera. Samples were analyzed using the Carl Zeiss LSM 510 confocal microscope.

DISCLOSURE

All the authors declared no competing interests.

ACKNOWLEDGMENTS

JAS was funded by GlaxoSmithKline (Clinician Scientist). FH is the Frederick G.L. Huetwell Professor, a Doris Duke Distinguished Clinical Scientist and was supported by grants from the National Institutes of Health.

REFERENCES

1. Gleeson JG, Keeler LC, Parisi MA *et al.* Molar tooth sign of the midbrain-hindbrain junction: occurrence in multiple distinct syndromes. *Am J Med Genet* 2004; **125A**: 125–134; discussion 117.
2. Joubert M, Eisenring JJ, Robb JP *et al.* Familial agenesis of the cerebellar vermis. A syndrome of episodic hyperpnea, abnormal eye movements, ataxia, and retardation. *Neurology* 1969; **19**: 813–825.
3. Parisi MA, Doherty D, Chance PF *et al.* Joubert syndrome (and related disorders) (OMIM 213300). *Eur J Hum Genet* 2007; **15**: 511–521.
4. Patel S, Barkovich AJ. Analysis and classification of cerebellar malformations. *AJNR Am J Neuroradiol* 2002; **23**: 1074–1087.
5. Keeler LC, Marsh SE, Leeflang EP *et al.* Linkage analysis in families with Joubert syndrome plus oculo-renal involvement identifies the *CORS2* locus on chromosome 11p12-q13.3. *Am J Hum Genet* 2003; **73**: 656–662.
6. Saar K, Al-Gazali L, Sztriha L *et al.* Homozygosity mapping in families with Joubert syndrome identifies a locus on chromosome 9q34.3 and evidence for genetic heterogeneity. *Am J Hum Genet* 1999; **65**: 1666–1671.
7. Valente EM, Salpietro DC, Brancati F *et al.* Description, nomenclature, and mapping of a novel cerebello-renal syndrome with the molar tooth malformation. *Am J Hum Genet* 2003; **73**: 663–670.
8. Hildebrandt F, Jungers P, Robino C *et al.* Nephronophthisis, medullary cystic kidney disease and medullary sponge kidney disease. In: Schrier RW (ed). *Diseases of the Kidney and Urinary Tract*. Lippincott Williams & Wilkins: Philadelphia, 2001 pp 475–485.
9. Wolf MT, Saunier S, O'Toole JF *et al.* Mutational analysis of the *RPGRIP1L* gene in patients with Joubert syndrome and nephronophthisis. *Kidney Int* 2007; **72**: 1520–1526.
10. Dixon-Salazar T, Silhavy JL, Marsh SE *et al.* Mutations in the *AHI1* gene, encoding jouberin, cause Joubert syndrome with cortical polymicrogyria. *Am J Hum Genet* 2004; **75**: 979–987.
11. Ferland RJ, Eyaid W, Collura RV *et al.* Abnormal cerebellar development and axonal decussation due to mutations in AHI1 in Joubert syndrome. *Nat Genet* 2004; **36**: 1008–1013.
12. Jiang X, Zhao Y, Chan WY *et al.* Deregulated expression in Ph+ human leukemias of AHI-1, a gene activated by insertional mutagenesis in mouse models of leukemia. *Blood* 2004; **103**: 3897–3904.
13. Hildebrandt F, Otto E. Molecular genetics of nephronophthisis and medullary cystic kidney disease. *J Am Soc Nephrol* 2000; **11**: 1753–1761.
14. Saunier S, Salomon R, Antignac C. Nephronophthisis. *Curr Opin Genet Dev* 2005; **15**: 324–331.
15. Otto E, Betz R, Rensing C *et al.* A deletion distinct from the classical homologous recombination of juvenile nephronophthisis type 1 (NPH1) allows exact molecular definition of deletion breakpoints. *Hum Mutat* 2000; **16**: 211–223.
16. Parisi MA, Bennett CL, Eckert ML *et al.* The *NPHP1* gene deletion associated with juvenile nephronophthisis is present in a subset of individuals with Joubert syndrome. *Am J Hum Genet* 2004; **75**: 82–91.
17. Tory K, Lacoste T, Burglen L *et al.* High NPHP1 and NPHP6 mutation rate in patients with Joubert syndrome and nephronophthisis: potential epistatic effect of NPHP6 and AHI1 mutations in patients with NPHP1 mutations. *J Am Soc Nephrol* 2007; **18**: 1566–1575.
18. Donaldson JC, Dempsey PJ, Reddy S *et al.* Crk-associated substrate p130(Cas) interacts with nephrocystin and both proteins localize to cell–cell contacts of polarized epithelial cells. *Exp Cell Res* 2000; **256**: 168–178.
19. Hildebrandt F, Otto E. Cilia and centrosomes: a unifying pathogenic concept for cystic kidney disease? *Nat Rev Genet* 2005; **6**: 928–940.
20. Olbrich H, Fliegauf M, Hoefele J *et al.* Mutations in a novel gene, *NPHP3*, cause adolescent nephronophthisis, tapeto-retinal degeneration and hepatic fibrosis. *Nat Genet* 2003; **34**: 455–459.
21. Watnick T, Germino G. From cilia to cyst. *Nat Genet* 2003; **34**: 355–356.
22. Mollet G, Silbermann F, Delous M *et al.* Characterization of the nephrocystin/nephrocystin-4 complex and subcellular localization of nephrocystin-4 to primary cilia and centrosomes. *Hum Mol Genet* 2005; **14**: 645–656.
23. Sparks AB, Rider JE, Hoffman NG *et al.* Distinct ligand preferences of Src homology 3 domains from Src, Yes, Abl, Cortactin, p53bp2, PLCgamma, Crk, and Grb2. *Proc Natl Acad Sci USA* 1996; **93**: 1540–1544.
24. Hildebrandt F, Otto E, Rensing C *et al.* A novel gene encoding an SH3 domain protein is mutated in nephronophthisis type 1. *Nat Genet* 1997; **17**: 149–153.
25. Utsch B, Sayer JA, Attanasio M *et al.* Identification of the first AHI1 gene mutations in nephronophthisis-associated Joubert syndrome. *Pediatr Nephrol* 2006; **21**: 32–35.
26. Valente EM, Silhavy JL, Brancati F *et al.* Mutations in CEP290, which encodes a centrosomal protein, cause pleiotropic forms of Joubert syndrome. *Nat Genet* 2006; **38**: 623–625.
27. Parisi MA, Doherty D, Eckert ML *et al.* AHI1 mutations cause both retinal dystrophy and renal cystic disease in Joubert syndrome. *J Med Genet* 2006; **43**: 334–339.
28. Sayer JA, Otto EA, O'Toole JF *et al.* A novel centrosomal protein, nephrocystin-6, is mutated in Joubert syndrome and activates transcription factor ATF4/CREB2. *Nat Genet* 2006; **38**: 674–681.
29. Donaldson JC, Dise RS, Ritchie MD *et al.* Nephrocystin-conserved domains involved in targeting to epithelial cell-cell junctions, interaction with filamins, and establishing cell polarity. *J Biol Chem* 2002; **277**: 29028–29035.
30. Benzing T, Gerke P, Hopker K *et al.* Nephrocystin interacts with Pyk2, p130(Cas), and tensin and triggers phosphorylation of Pyk2. *Proc Natl Acad Sci USA* 2001; **98**: 9784–9789.
31. Bernard P, Fleming A, Lacombe A *et al.* Wnt4 inhibits beta-catenin/TCF signaling by redirecting beta-catenin to the cell membrane. *Biol Cell* 2007; **100**: 167–177.
32. Morgan D, Eley L, Sayer J *et al.* Expression analyses and interaction with the anaphase promoting complex protein Apc2 suggest a role for inversin in primary cilia and involvement in the cell cycle. *Hum Mol Genet* 2002; **11**: 3345–3350.
33. Eley L, Yates LM, Goodship JA. Cilia and disease. *Curr Opin Genet Dev* 2005; **15**: 308–314.
34. Gabow PA, Kaehny WD, Johnson AM *et al.* The clinical utility of renal concentrating capacity in polycystic kidney disease. *Kidney Int* 1989; **35**: 675–680.
35. Dalgaard OZ. Bilateral polycystic disease of the kidneys; a follow-up of two hundred and eighty-four patients and their families. *Acta Med Scand Suppl* 1957; **328**: 1–255.
36. Martinez-Maldonado M, Yium JJ, Eknoyan G *et al.* Adult polycystic kidney disease: studies of the defect in urine concentration. *Kidney Int* 1972; **2**: 107–113.
37. Gardner Jr KD. Juvenile nephronophthisis and renal medullary cystic disease. *Perspect Nephrol Hypertens* 1976; **4**: 173–185.
38. Bodaghi E, Honarmand MT, Ahmadi M. Infantile nephronophthisis. *Int J Pediatr Nephrol* 1987; **8**: 207–210.
39. Gattone II VH, Maser RL, Tian C *et al.* Developmental expression of urine concentration-associated genes and their altered expression in murine infantile-type polycystic kidney disease. *Dev Genet* 1999; **24**: 309–318.
40. Gattone II VH, Wang X, Harris PC *et al.* Inhibition of renal cystic disease development and progression by a vasopressin V2 receptor antagonist. *Nat Med* 2003; **9**: 1323–1326.
41. Torres VE, Wang X, Qian Q *et al.* Effective treatment of an orthologous model of autosomal dominant polycystic kidney disease. *Nat Med* 2004; **10**: 363–364.
42. Torres VE. Therapies to slow polycystic kidney disease. *Nephron Exp Nephrol* 2004; **98**: 1–7.